

Power System Redundancy Design Trends for All-Electric eVTOL Quadrotors

George L. Thomas¹ and Brian P. Malone²
NASA Glenn Research Center, Cleveland, Ohio, 44135

Electrical vertical takeoff and landing (eVTOL) vehicles promise to enable a variety of new local and intraregional air transport missions. However, there are significant challenges that must be solved to enable their use. One challenge is the relatively low reliability of power components (e.g. motors, power electronic devices, and batteries). No clear development path to create reliable eVTOL power systems has been articulated in the literature, though it is generally assumed redundancy is part of the solution. This work proposes an analysis process to examine the redundancy design space and select mass optimal designs for eVTOL power systems. The process is applied to a six passenger quadrotor vehicle, and results are used to highlight redundancy design trends for this class of vehicle. This process and associated data can help vehicle designers more effectively develop eVTOLs that meet reliability requirements.

I. Introduction

ELECTRIC vertical takeoff and landing (eVTOL) vehicles are expected to enable a variety of new missions, particularly local and intraregional air travel. A term for these missions is advanced air mobility (AAM) [1]. eVTOLs are especially promising for these missions because vertical takeoff capability enables operation in localized and urban spaces without access to runways, and propulsion system electrification enables design flexibility (e.g. distributed propulsion) that can increase vehicle efficiency, and facilitates use of low carbon or renewable power for flight. However, electrified propulsion is still largely an open research and development area, with significant investment from industry and government agencies worldwide.

A key challenge to electrified propulsion for eVTOLs and most other classes of aircraft is the relatively low reliability of the necessary power components. Previous studies have identified electric machines, power electronics, and batteries as weak links for propulsion system reliability based on historical data [2]. There are several approaches to improve the reliability of these components. One is to run these devices at lower temperature or otherwise increase their operating temperature margin, because reduced operating temperatures are correlated with significantly longer lifespans of electrical power equipment [3]. This may be done by using higher temperature rated components (e.g. high temperature insulation materials, wide bandgap power electronics instead of silicon, etc), by reducing losses within the components, or through more aggressive thermal management, though the latter comes with costs in terms of mass and load power. Another is to reduce electrical stress on the devices, which may include adhering to power quality standards that bound these stresses [4], and increasing margin for electrical variables in the design, although additional margin may incur performance costs.

Redundancy is another key approach towards increasing reliability and can be applied at the component or at the system level. Aircraft feature redundancy throughout, including in engine control systems [5] as well as fly-by-wire systems for vehicle control [6]. This work focuses on how redundancy can be used in the power system design in the all-electric NASA Revolutionary Vertical Lift Technology (RVLT) six passenger quadrotor concept vehicle (Quad6) to meet a representative reliability requirement. A rendering of this vehicle, first published in Ref. [7], is given in Figure 1.

¹ Electrical Engineer, Power Management and Distribution Branch, george.l.thomas@nasa.gov, AIAA Member.

² Electrical Engineer, Power Management and Distribution Branch, brian.p.malone@nasa.gov, AIAA Member.



Figure 1: Rendering of the RVLT six passenger quad.

It is expected that electrified propulsion power systems must feature some amount of redundancy. US patents and patent applications have been published describing possible power system redundancy designs, and describe many power system architecture considerations for multirotors, but these do not include analysis on the designs showing intent to meet reliability requirements, and they do not explore redundancy design space trends in detail [8, 9]. Little more has been published on this topic. This paper seeks to address this lack of published information by presenting a process to identify mass optimal redundancy designs that meet a given set of reliability requirements. This paper also applies this process to the RVLT Quad6 concept vehicle and includes a discussion of design trends and results. This methodology and data will help inform vehicle systems designers (especially in startups and those new to the field [10]) about redundancy design trends and practice, which will help them develop plans to meet relevant reliability requirements early on and avoid costly redesign cycles.

Regarding reliability requirements, note that the US Federal Aviation Administration (FAA) Advisory Circular (AC) 25.1309-1 and its revisions advise that catastrophic failure conditions must be extremely improbable (10^{-6} to 10^{-9} or less depending on aircraft class) and that no single failure will result in a catastrophic failure condition, in order for an aircraft to comply with the Federal Aviation Regulation (FAR) 25.1309 airworthiness standard [11]. From this, one can infer that all safety critical systems must be at least single fault tolerant. However, the FAA catastrophic failure probability requirement for eVTOLs has been ambiguous in the past due to the lack of definition and changing type classification for these vehicles [12]. On the other hand, the European Union Aviation Safety Agency (EASA) SC-VTOL-01 requires a failure rate of 10^{-9} failures per flight hour for special condition certification of small VTOLs [13]. This work assumes requirements of single fault tolerance and a vehicle level catastrophic failure rate of 10^{-9} failures per flight hour consistent with assumptions in previous studies [2]. Further, only catastrophic failures of power system components are considered. Power system reliability requirements are presented later in the text, based on the above assumptions.

Section II describes the vehicle studied in this work. Section III covers the reliability analysis approach that was used in this work, with details on the associated reliability and mass models. Section IV discusses results and trends found in the study. Section V provides summary and conclusions.

II. Vehicle Assumptions

For this study, this vehicle is assumed to require 160 kW shaft power at each rotor. It is also assumed the power distribution architecture for the vehicle is a 1 kV DC radial system. The main bus is assumed to be battery backed and unregulated to avoid adding additional converters or regulators (and thus additional mass) between the battery and the main bus. All power for flight is sourced from Li-ion batteries, and the main bus power is delivered to the motors via inverters or variable speed motor drives which are fed by 5 meter cable runs. The baseline power system architecture (zero fault tolerant, with no redundant components) is shown in Figure 2.

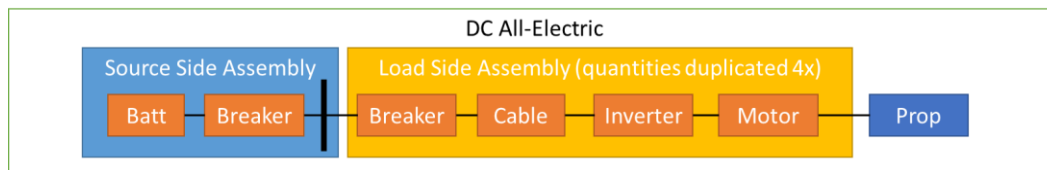


Figure 2: Power system for the all-electric six passenger quad.

Performance and reliability technology assumptions for this vehicle are given in Table 1.

Table 1: Component technology assumptions.

Variable	Value	Variable	Value
Minimum Required Rotor Hover Power (kW)	160	Battery Specific Energy (Wh/kg)	400
Mission Duration (h)	1	Battery Design Energy (kWh)	275
Pylon / Cable Length (m)	5	Nominal Battery Voltage (V_{dc})	1000
Electric Machine Specific Power (kW/kg)	13	Nominal Battery Efficiency at Full Load	0.94
Electric Machine Efficiency	0.96	Electric Machine Failure Rate (failures/hr)	10^{-6}
Power Electronics Specific Power (kW/kg)	9	Power Electronics Failure Rate (failures/hr)	$5 \cdot 10^{-6}$
Power Electronics Device Efficiency	0.95	Battery Failure Rate (failures/hr)	$3.45 \cdot 10^{-6}$

The efficiency, specific power, and specific energy technology values are based on assumptions about near-term future technology projected by the RVLТ project [7]. The component failure rates are based on legacy constant failure rate (exponential distribution) models of the associated components and are assumed for this work to be accurate to within an order of magnitude [14, 15]. The authors expect these electric machine and power electronics failure rates may be conservative (i.e. overestimated), assuming proper engineering margin is built into the associated designs and quality parts are used, and so one may expect the system failure rates predicted in this work to be overestimated as well. The battery-backed main bus nominal voltage of 1000 V is chosen to be a conservative medium voltage value consistent with both RVLТ hardware test capability goals and previous work [16]. Lastly, the propulsion system is assumed to be RPM controlled and does not feature cross shafting. It is assumed that the vehicle must maintain the full 160 kW rotor power capability at all four rotors and at all times in order to safely end a mission. Thus reliability in this paper is defined as the probability that all four rotors maintain a 160 kW power capability over the course of a full mission duration.

III. Modeling and Analysis Approach

This work uses the Electrical Power System – Sizing and Analysis Tool (EPS-SAT) to size the candidate system designs to the required load power, and estimate the associated system masses [17, 18]. New reliability engineering functions were added to EPS-SAT to enable calculating power system reliability and catastrophic failure rate based on the system architecture and assumed component failure rate data. In this work, the masses and failure rates of multiple power system design variants featuring different redundancy schemes are calculated. The redundancy design problem can be casted as an optimization problem in these two variables (system mass and failure rate), and a Pareto optimal (non-dominated) set of redundancy design solutions can be identified. Non-dominated design solutions are those that cannot be improved in any one objective function dimension without compromising at least one other dimension, and dominated design solutions are suboptimal ones that can be improved upon in multiple objective dimensions. The Pareto front represented by these solutions captures the tradeoff design trend between mass and reliability. Note that design solutions will be subject to one or more reliability constraints per regulations. The solution to be selected from the design space should be the lowest mass solution that meets the reliability constraints, because the lowest mass solution should enable a higher performing overall vehicle design. Figure 3 shows a visualization of the redundancy design space in mass and failure rate, showing dominated and non-dominated solutions, Pareto front, a reliability constraint, and the mass optimal feasible solution subject to the constraint.

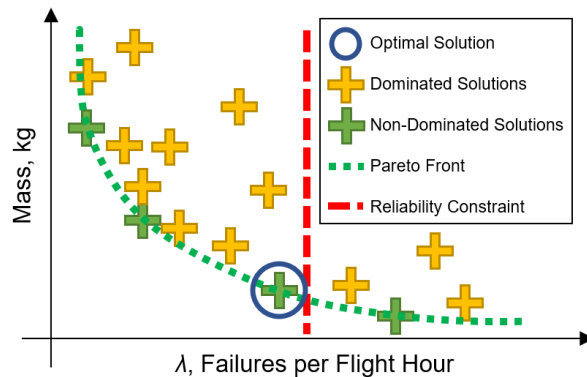


Figure 3: Redundancy design space for a hypothetical system.

In this work, a failure rate constraint of 10^{-10} catastrophic power system failures per flight hour was chosen, assuming this will support the EASA SC-VTOL-1 vehicle level failure rate of 10^{-9} failures per flight hour [2]. The remainder of this section discusses details of the reliability and mass models used in this work.

A. Reliability Modeling

In EPS-SAT, single (non-redundant) component reliabilities are calculated from the component failure rates using the exponential distribution definition

$$R = e^{-\lambda T} \quad (1)$$

where R is the component reliability, λ is the component's assumed constant failure rate, and T is a period of time of interest in flight hours. In our case, T is taken to be the maximum time duration of a given mission, which is assumed for this initial study to be 1 hour for this vehicle. Once component reliabilities are obtained, the system reliability and failure rates can be calculated as series and parallel combination of the component reliabilities and failure rates. For series combinations of components, the total failure rate is the sum of the component failure rates, and the total reliability is the product of the reliabilities. The reliability for k -out-of- n parallel redundant systems is given by the following function

$$R_{k\text{-out-of-}n}(R, k, n) = 1 - \sum_{m=0}^{k-1} \binom{n}{m} (1-R)^{n-m} R^m \quad (2)$$

where n is the number of redundant parallel elements, k is the number of healthy elements required for mission success, and m is a summation index used in the expression [19]. Once the reliability of a redundant combination of elements is calculated, the failure rate of the redundant set of components is calculated by the inverse of Eqn. (1).

$$\lambda = -\frac{\ln(R)}{T} \quad (3)$$

The generalized redundancy architecture for the all-electric Quad6 power system is broken down into primary and secondary power systems and integrated into an end-to-end power system as illustrated in Figure 4.

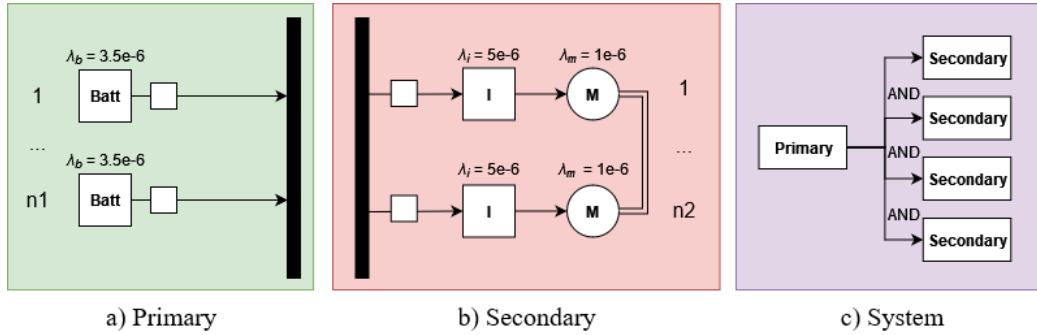


Figure 4: Reliability block diagrams for a) the primary power system, b) the secondary power system, and c) the entire power system.

The primary power system is composed of a number of parallel batteries as shown in Figure 4a. The reliability of the k_1 -out-of- n_1 redundant primary power system can be calculated as

$$R_{pri} = R_{k\text{-out-of-}n}(R_b, k_1, n_1) \quad (4)$$

where k_1 and n_1 are the redundancy parameters for the primary system and R_b is the reliability of one battery. Second, each rotor is driven by a number of parallel motor/inverter strings, and each parallel set is referred to in this paper as a secondary power system, as shown in Figure 4b. Because each secondary string features a series inverter and motor, the secondary system reliability can then be calculated as

$$R_{sec} = R_{k\text{-out-of-}n}(R_i R_m, k_2, n_2) \quad (5)$$

where k_2 and n_2 are the redundancy parameters for the secondary system, and R_i and R_m are the reliabilities of one inverter and one motor. Note that the product of R_i and R_m is the reliability of a single one of the redundant secondary strings.

The overall power system is composed of a primary system, and four secondary power systems which each drive one of the four rotors as shown in Figure 4c. It is assumed the power system must be capable of delivering the full 160 kW shaft power at all times to all four rotors for the mission to be successful, meaning that none of the four secondary systems can fail for a successful mission. Given these assumptions, the full system reliability can then be written as

$$R_{sys} = R_{pri}R_{sec}^4 \quad (6)$$

The parallel inverters in Figure 4b may represent multiple separate inverters or may represent multiple inverter modules or cards that could be packaged in a single box. Likewise, multiple motors in Figure 4b may represent multiple separate motors, or multiple independent modular windings. The modular approach will likely be more mass efficient for both, and so may be preferred.

Figure 4 shows all of the primary strings tied in parallel to a single main bus. In order for the reliability equations above to be valid in this case, it must be assumed that proper circuit protection is present and devices adhere to a power quality standard such that failures of one of the redundant primary strings will not affect any of the secondary strings and vice versa. This must be the case so that the failure rates of the redundant primary and secondary systems are independent from one another. In an alternative design, each primary string could power its own independent, isolated bus, and each secondary could then draw power equally from all of these isolated busses. This design approach should improve reliability in practice, however it may be challenging to design the inverters to accept power from each of the isolated primary busses. It is assumed for this work that a single bus is equivalent in terms of mass and failure rate to the alternative multiple isolated bus approach, so selection between these approaches is left for future work. All redundant components are assumed in this paper to “operate hot” and are nominally assumed to equally share load power. Architectures based on load sharing redundancy tend to have higher common cause failure rates than architectures that feature redundant backup systems that normally are not operational. This is because when a load sharing element goes offline, the remaining elements see an instantaneous increase in load, and higher loads are associated with higher component failure rates. Also, since these parallel load sharing components all see the same bus, any power quality phenomenon such as voltage surge will stress all redundant parts equally and such a phenomenon could be a common cause of potential failures. For this work, these common cause failures are accounted for using a beta factor model, with beta assumed to be 0.1. This value is reported to be a conservative beta factor assuming good engineering practice is followed [20]. Note that beta factor models are simplistic and a higher fidelity model of common cause failure rates could be adapted for future work.

B. Mass Modeling

Masses for single components in this study are calculated by dividing the component design power (a function of the rotor maximum load requirement) by the specific power assumed in Table 1. The mass of a k-out-of-n redundant array of parallel components is calculated as expression

$$m_{k\text{-out-of-}n} = nfm_{1\text{-out-of-}1} \quad (7)$$

where f is the fractional design power that each redundant component in the array is designed to. In this work, it is assumed $f = 1/k$, which results in the minimum component power rating needed for k components in parallel to equal the design power.

Note that this mass modeling approach is fairly simplistic. For one, it does not attempt to predict how the various subsystem masses within a given component will vary with redundancy design variables (e.g., structural, bearings, shaft, back iron, and windings for a motor). Attempts to account for this are difficult because the manner in which these masses vary depends greatly on how the component is designed, and electrified propulsion component designs themselves vary greatly. This model also neglects the fact that as the number of parallel redundant components increases, the amount of overhead mass should also increase (e.g., additional wiring harnesses for the additional redundant components, additional enclosures, etc). For instance, this model predicts 1-out-of-2 redundant systems to have the same mass as 2-out-of-4, which may not be true in reality—one would expect the 2-out-of-4 redundant system to have more overhead mass as it is a more complex system with a larger number of parts. The actual overhead mass for redundant systems should depend strongly on engineering and packaging decisions made in the design process and thus is hard to estimate. In addition, little data has been published on this overhead mass, complicating efforts to model

it. Ultimately, this simplified mass modeling approach was taken to avoid making too many assumptions about the design which could limit the general applicability of the work and overcomplicate the analysis effort.

IV. Results and Discussion

A study was conducted where the redundancy design variables for the primary (k_1 and n_1) and secondary (k_2 and n_2) systems were varied. Each component in a k -out-of- n redundant system is sized to a power level equal to $1/k$ times the total power required for the whole set of redundant components. This means that k elements in parallel (the bare minimum for full capability operation) will be capable of up to the total required power. Realistic designs may size components to powers greater than $1/k$, as this represents design margin which is often desired or required in real systems.

In this study, n_1 and n_2 were varied from 0 to 4. For each value of n_1 , k_1 was varied from 1 to n_1 (and likewise with k_2 and n_2). This results in an exhaustive search over the redundancy design space for values of n_1 and n_2 up to 4. Given that this study is an exploration of a design space in four variables (n_1 , n_2 , k_1 , and k_2), with two objective variables (system mass and failure rate), the data is not straightforward to analyze. The approach taken in this work is to draw multiple mass versus failure rate curves with the primary power system redundancy parameters held constant while the secondary system parameters are varied for the stated values of k_2 and n_2 . Figure 5 provides an example by showing total power system mass (including battery, cables, motors, and inverters) versus the log of the system catastrophic failure rate for an architecture with a non-redundant primary power system ($n_1 = k_1 = 1$) and variable secondary power system redundancy designs (n_2 and k_2 varied).

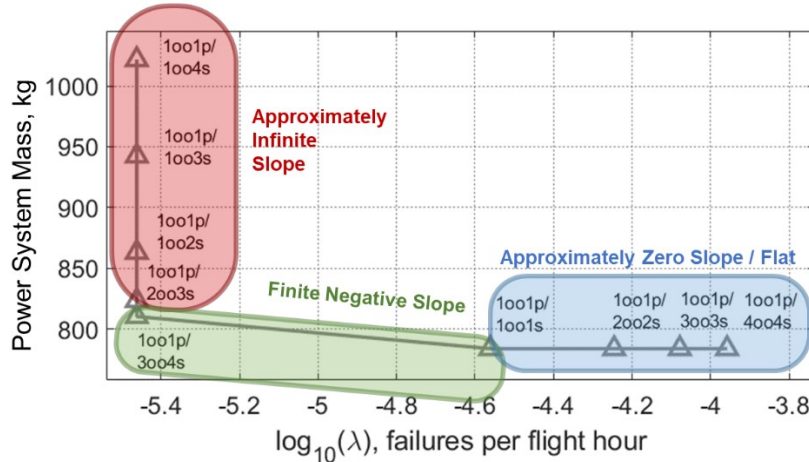


Figure 5: Mass versus failure rate trend as secondary system redundancy is varied, highlighting parts of design trend.

Markers are drawn in Figure 5 for each design solution, and the redundancy design parameters associated with a particular solution are indicated in abbreviated text next to each marker. For example, “1001p” represents the non-redundant primary system design analyzed in this figure. Likewise, “2003s” corresponds to a 2-out-of-3 redundant secondary—that is, three redundant strings or sets of components that are sized and operated such that only two of these is needed for full operation. It should be noted that none of the solutions in Figure 5 meet the reliability constraint, indicating some degree of redundancy is needed in the primary power system.

Each of the curves for a given primary redundancy design in Figure 5 includes a region where the mass versus failure rate trend is flat or approximately zero slope (as shown in the blue circle), a region with finite negative slope (green circle), and a region with approximately infinite negative slope (red circle). The flat part of the design trend, in blue, is where the secondary system has a lower reliability than the primary and is the limiting factor for system reliability. In this case a higher redundancy allocation to the secondary will improve reliability without adding mass. The red, near infinite negative slope region is where the primary system reliability is significantly lower than the secondary system and dominates the trend. In this part of the trend, further improvements to system reliability require more redundancy allocation to the primary system, or alternatively, one can reduce secondary system redundancy to reduce mass without an impact on reliability. Finally, the finite slope region corresponds to where the primary and secondary system have reliabilities that are fairly close to each other. This region is where one is most likely to find a mass optimal overall design solution and corresponds to design solutions with well balanced redundancy allocation.

Figure 6 shows mass versus failure rate curves for multiple primary system redundancy designs. Each colored solid line plotted in the figure shows the mass versus failure rate trend for one primary system redundancy design while the secondary system redundancy design is varied. Primary system redundancy design values are indicated for each curve in the legend via abbreviated text (*koon*). The dotted black line shows the Pareto front connecting all non-dominated design solutions, and the red dashed line shows the reliability constraint of 10^{-10} failures per flight hour. Note that some primary system designs (e.g. 2oo2 and 3oo3) are omitted from Figure 6 as they tend to be suboptimal.

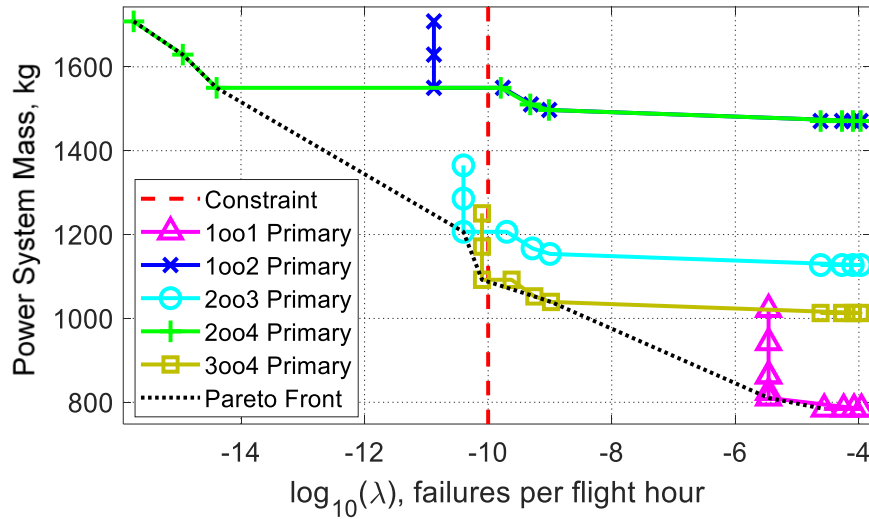


Figure 6: Mass versus failure rate trends for several primary power system redundancy designs as the secondary design is varied.

This data shows that to minimize mass, the primary system should be 3oo4 redundant. The data also shows that a 2oo3 redundant primary system has a comparable system failure rate while only being about 10% heavier and is a good alternative solution. The 1oo1 (non-redundant) solution weighs 784 kg, while the best case 2oo3 and 3oo4 primary system designs weigh 1092 and 1206 kg respectively. This corresponds to a 39% increase in mass to meet reliability constraints versus the non-redundant solution. Note that a powertrain designer may want to select the 2oo3 redundant primary design instead of a 3oo4, despite the additional mass, due to the fact that 2oo3 should result in a simpler, more conventional system. Ultimately, both primary system design solutions should be considered further.

While Figure 6 is useful for indicating overall trends and analysis of primary system redundancy, it does not indicate secondary system design solutions due to lack of space on the graphic. Figure 7 shows the mass versus failure rate data for the 2oo3 and 3oo4 primary systems and indicates both the primary and secondary system redundancy variables of each solution (e.g., 2oo3p/1oo4s on the graphic represents a 2oo3 redundant primary, and 1oo4 redundant secondary).

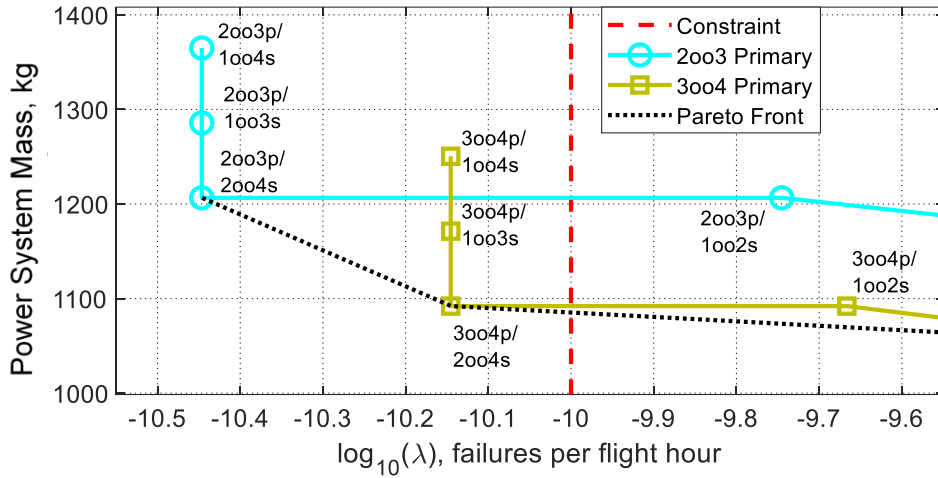


Figure 7: Mass versus failure rate for select redundancy design solutions closest to the reliability constraint.

Figure 7 shows that the 2004 secondary system design is mass optimal for both the 2003 and 3004 primary system designs. Note that this secondary system design tends to sit at the bottom of the infinite slope region of each of these curves. This indicates that secondary system solutions more reliable than 2004 (i.e., 1003 and 1004) represent excessive, unnecessary redundancy allocated to the secondary system.

This analysis was conducted again on a variant of the vehicle assumed to include cross shafting and collective control instead of RPM control without cross shafting. Mass of the gearbox, cross shafting, and collective mechanisms are neglected in this study for simplicity however these are not insignificant in general. This analysis was conducted to see how different the trend is for these two different propulsion system concepts, given that there is an ongoing debate about the drawbacks and benefits for each in the literature, with no clear winner identified in general. With cross shafting, the propulsion system no longer needs the full 160 kW of motor capability active at each rotor station. Instead, it is assumed it only needs 160 kW total per rotor, no matter where it is generated. This is because the cross shafting allows rotors to be driven with mechanical power generated at other rotor stations. This means that instead of Eqn (4), the total secondary reliability is given by

$$R_{sec(cross)} = R_{k-out-of-n}(R_l R_m, 4k_2, 4n_2) \quad (8)$$

and instead of Eqn (5), the system reliability is given by

$$R_{sys(cross)} = R_{pri} R_{sec(cross)} \quad (9)$$

Figure 8 illustrates why this is the case by looking at the full collection of secondary strings at all four rotors, assuming a 1002 redundant secondary system. For the non cross shafting system on the left of Figure 8 it can be seen that one of the two secondary strings at the front left rotor may fail and the remaining one will be able to provide full power to that rotor (noting that 1002 means each secondary string is sized to the full rotor load of 160 kW). However, without cross shafting, if both fail, the success criteria will not be met, and the result is a catastrophic system failure. On the other hand, the cross shafting system shown on the right of Figure 8 represents one large redundant collection of secondary strings distributed across the vehicle, instead of four smaller ones. In this system, losing all motoring capability at one location is not significantly worse than losing the same amount of capability distributed across multiple locations.

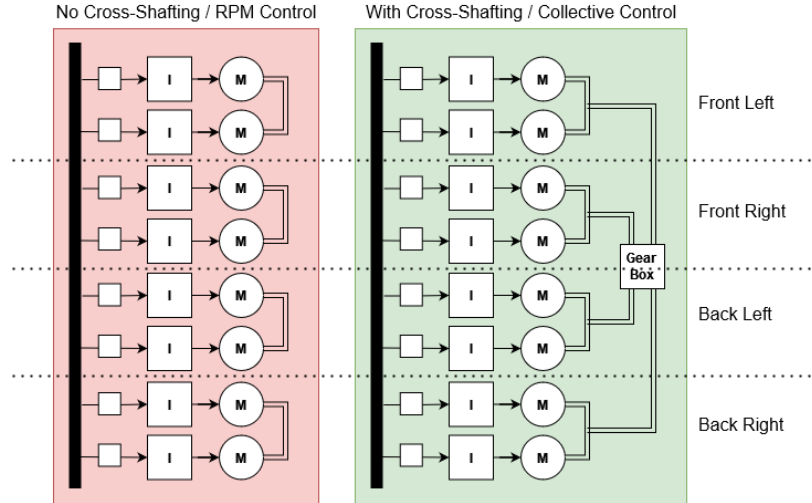


Figure 8: Block diagram showing shaft connections (double parallel lines) between motors for the non cross-shaft quadrotor powertrain concept (left) and for the cross-shaft powertrain (right).

In order to capture the reliability differences between these variant powertrains, Figure 9 shows the trend for 2003 primary system designs comparing the baseline non-cross shafted concept with the cross shafted one. The data shows that the collection of secondary systems in the cross shafting concept is at least as reliable as the non-cross shafting version, and in multiple cases is more reliable.

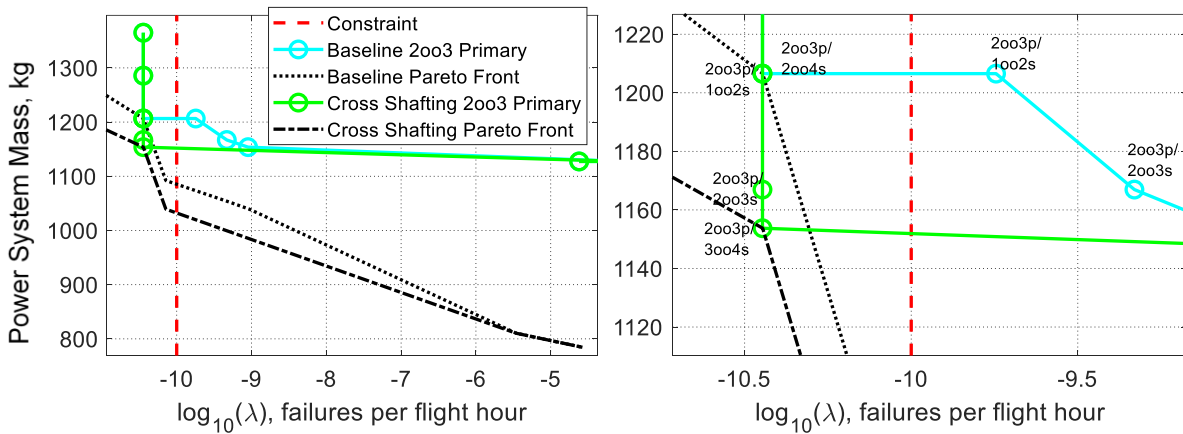


Figure 9: Mass versus failure rate trend comparing baseline concept and concept with cross shafting, shown both over a significant portion of the design space (left) and zoomed in on the constraint (right).

The power system masses (neglecting gearing and shafting) for the baseline and cross shafting concepts are the same, however the trend is slightly more favorable for the cross shafting concept due to the fact that its secondary system generally has lower failure rate than the baseline for the same designs values (n_1 , n_2 , k_1 , and k_2). Figure 9 shows that the cross shafting concept benefits from a lower secondary system redundancy allocation compared to the baseline, indicating that it needs less redundancy. For instance, the cross shafting concept is in its infinite slope region for the 2003p/2003s redundancy design (indicating the level of secondary redundancy is excessive), whereas for the baseline, the 2003p/2003s design is still within the finite slope region (indicating this level of redundancy is a good allocation).

The optimum power system mass for the cross shafting concept is 1153 kg vs 1206 kg for the baseline, resulting in a 4% decrease. This may not be a significant enough decrease in mass to warrant the additional complexity of the cross shafting especially since cross shafting will add weight that may offset the redundancy trend benefit. However other considerations for the drivetrain should ultimately be taken into account including the handling and ride qualities

of the two concepts. Mainly, there are concerns that RPM control of vehicles with large rotors may be difficult or impossible because the large rotor inertias make it challenging to meet maneuverability requirements.

V. Conclusions

This paper shows an electrified propulsion power system redundancy design analysis process and applies it to the RVLT all-electric six passenger quadrotor. The process can help conceptual design and analysis teams select power system redundancy architectures by identifying mass optimal designs and highlighting design trends. The implementation of this method in the EPS-SAT tool will help NASA conduct future mass-redundancy tradeoff studies in a single integrated tool, enabling it to develop conceptual power system designs with appropriate levels of redundancy and more accurately estimate associated masses needed for that redundancy. The data from this work shows that for the six passenger quadrotor, 3004 and 2003 are optimal primary power system redundancy designs (i.e., the batteries that make up the main bus). Likewise, 2004 is the mass optimal redundancy design for the secondary power system (i.e., the inverters and motors that drive the rotors). This study shows that the required level of redundancy to meet reliability constraints results in 39-54% additional power system mass compared to a non-redundant (1001) system. A powertrain with cross shafting was also shown to be more reliable, however the overall benefit in terms of optimal power system mass (4% or less) may not be enough to recommend cross shafting over individual RPM controlled rotors. Note that fidelity may be added to the mass and reliability models in future work. Also note that maintainability was ignored in this study and can be addressed in future work.

Acknowledgments

The authors would like to acknowledge the Revolutionary Vertical Lift Technology (RVLT) project under the Aerospace Research Mission Directorate (ARMD) that has supported this work.

References

- [1] "Advanced Air Mobility National Campaign Overview," NASA [website], URL: <https://www.nasa.gov/aeroresearch/aam/description/> [retrieved 21 May 2022].
- [2] Darmstadt, P., et. al., "Hazards Analysis and Failure Modes and Effects Criticality Analysis (FMECA) of Four Concept Vehicle Propulsion Systems," The Boeing Company, NASA CR-2019-220217, June 2019.
- [3] Lakshminarayanan, V. and Sriraam, N., "The Effect of Temperature on the Reliability of Electronic Components", *2014 IEEE International Conference on Electronics, Computing and Communication Technologies (IEEE CONECCCT)*, Bangalore, India; February 2014
- [4] Ae-10 High Voltage Committee, "Aircraft High Voltage DC Power Quality Standard [Work in Progress]" SAE Aerospace Standard AS7499, 2019
- [5] Kniat, J. and Bluish, J., "An Application of Redundancy in Digital Electronic Engine Control," SAE Technical Paper 801200, 1980
- [6] Bumby, E., "Redundancy Management for Fly-by-Wire Systems," *AIAA Guidance and Control Conference*, August 1972. <https://doi.org/10.2514/6.1972-884>
- [7] Silva, C., Johnson, W., Solis, E., and Patterson, M., "VTOL Urban Air Mobility Concept Vehicles for Technology Development," AIAA Aviation Forum, Atlanta, GA, June 25-29, 2018.
- [8] Bevirt, J., Stoll, A., van der Geest, M., MacAfee, S., Ryan, J., "Electric Power System Architecture and Fault Tolerant VTOL Aircraft Using Same" U.S. Patent Application No. US20200010187A1, 2020.
- [9] Melack, J., "Systems And Methods For Power Distribution In Electric Aircraft" U.S. Patent No. US11465764 B2, 2022.
- [10] "eVTOL Aircraft Directory," Vertical Flight Society [website], URL: <https://evtol.news/aircraft> [retrieved 24 May 2022].
- [11] US Federal Aviation Administration, "FAA Advisory Circular 25.1309-1A - System Design and Analysis," 1988 URL: https://www.faa.gov/regulations_policies/advisory_circulars/index.cfm/go/document.information/documentid/22680 [retrieved 11 November 2022]
- [12] Brinkmann, P., "AAM companies press FAA to clarify pathway for powered-lift certification" *Aerospace America*, September 23, 2022. URL: <https://aerospaceamerica.aiaa.org/aam-companies-press-faa-to-clarify-pathway-for-powered-lift-certification/> [retrieved 11 November 2022].
- [13] European Union Aviation Safety Agency (EASA), "Special Condition for Small-Category VTOL Aircraft" EASA Special Condition, SC-VTOL-01, 2019 URL: <https://www.easa.europa.eu/sites/default/files/dfu/SC-VTOL-01.pdf> [retrieved 11 November 2022]
- [14] Lalli, V., et al., "Reliability and Maintainability (RAM) Training," NASA/TP-2000-207428, July 2000.
- [15] Tang, Q., Shu, X., Zhu, G., Wang, J., and Yang, H., "Reliability Study of BEV Powertrain System and Its Components – A Case Study," *Processes* 2021, 9(5), 762. <https://doi.org/10.3390/pr9050762>

- [16] Thomas, G., Chapman, J., Alencar, J., Hasseeb, H., Sadey, D., and Csank, J., "Multidisciplinary systems analysis of a six passenger quadrotor Urban Air Mobility vehicle powertrain,". *AIAA Propulsion and Energy Forum*. August 2020. <https://doi.org/10.2514/6.2020-3564>
- [17] Hanlon, P., Thomas, G., Csank, J., and Sadey, D., "A Tool for Modeling and Analysis of Electrified Aircraft Power Systems," *2019 AIAA/IEEE Electric Aircraft Technologies Symposium (EATS)*, 2019, pp. 1-16, doi: 10.2514/6.2019-4403.
- [18] "Electrical Power System - Sizing and Analysis Tool (EPS-SAT) (LEW-20017-1)," NASA Software Catalog [website], URL: <https://software.nasa.gov/software/LEW-20017-1> [retrieved 24May2022].
- [19] Nakashima, K., Matznaga, H., Ueda, Y., Yamato, K., "Optimal Design of Redundant Systems for Improving Fail-Safe Characteristics" *Computers and Mathematics with Applications*, Vol. 24, No. 1/2, pp. 109-117, 1992.
- [20] Jones, H., "Common Cause Failures and Ultra Reliability," *42nd International Conference on Environmental Systems*, 15 July 2012 - 19 July 2012, San Diego, California, <https://doi.org/10.2514/6.2012-3602>